Extreme Mechanics Letters 53 (2022) 101720

Contents lists available at ScienceDirect

Extreme Mechanics Letters

journal homepage: www.elsevier.com/locate/eml

Bioinspired multimodal soft robot driven by a single dielectric elastomer actuator and two flexible electroadhesive feet

Yaguang Guo [a], Jianglong Guo [b], Liwu Liu [a,*], Yanju Liu [a], Jinsong Leng [c,*]

[a] Department of Astronautical Science and Mechanics, Harbin Institute of Technology, P.O. Box 301, No. 92 West Dazhi Street, Harbin 150001, China
[b] School of Science, Harbin Institute of Technology (Shenzhen), Shenzhen, 518055, China
[c] Center for Composite Materials and Structures, Science Park of Harbin Institute of Technology, P.O. Box 3011, No. 2 YiKuang Street, Harbin 150080, China

ARTICLE INFO

Article history:
Received 22 December 2021
Received in revised form 4 March 2022
Accepted 27 March 2022
Available online 6 April 2022

Keywords:
Bioinspiration
Soft robotics
Dielectric elastomer actuator
Flexible electroadhesive

ABSTRACT

Locomotion is an important ability of animals and bioinspired mobile robots. It is, however, challenging for current soft mobile robots to achieve multimodal locomotion within a simple structure. Inspired by caterpillars, we combine a two-degree-of-freedom (2-DOF) dielectric elastomer actuator (DEA) and two flexible electroadhesives (EAs) to form the multimodal soft robot. The 2-DOF DEA was regarded as the deformable body that can elongate, contract, and bend. The EAs, fabricated by a cost-effective cut-transfer method, acted as two feet that can provide required and sufficient frictions whilst moving on different surfaces. Both the DEA and EA were experimentally characterized. As a result, we developed a caterpillar inspired soft robot capable of multimodal turning, crawling, and climbing. The robot was able to crawl at a speed of 2.38 mm/s, achieve two turning modes, climb at a speed of 2.30 mm/s, and can still function after 10000 operation cycles. The robot was further demonstrated to carry a micro camera for inspection tasks in a narrow tunnel, and it may be possible to deploy the robot on satellites for detection uses. This study provides a new insight for the design of bioinspired soft robots with multimodal locomotion capabilities.

© 2022 Elsevier Ltd. All rights reserved.

1. Introduction

Locomotion is essential for the survival of natural creatures (such as caterpillars and inchworms) so that they can crawl on challenging natural surfaces (such as branches and leaves) to find food and avoid enemies. Designing robots with such locomotion capabilities has always been a key challenge. Traditional robots can imitate the locomotion of natural creatures, but their structures and driving modes are relatively complex. Their flexibility and adaptability are also limited because most of them are made of rigid materials. Recently, soft robots, like natural creatures, made of all-soft or soft-rigid materials, have been extensively studied and exploited due to their excellent abilities, including inherent flexibility, agility, large and continuum deformation, and infinite degrees of freedom [1–5]. This makes them more promising to replicate these appealing locomotion capabilities.

Various kinds of soft robots with different actuation technologies and locomotion mechanisms have been developed. Pneumatic actuation has been the most common driving technology [6,7]. Other stimuli response smart materials have also been employed to develop soft robots, such as shape memory alloys (SMA) [8,9], shape memory polymers (SMP) [10,11], dielectric elastomers (DEs) [12,13], ionic polymer metal composites (IPMC) [14], liquid crystalline elastomers (LCE) [15,16], hydrogels [17,18], etc. Thanks to their inherent soft, large deformation, fast response, and high energy density, dielectric elastomer actuators (DEAs) are promising actuators for soft robots and have been employed in many kinds of soft mobile robots [19–29]. Most of the existing studies generally focused on imitating the forward motion of natural creatures, as shown in Table 1.

For the insect-sized soft robot with three legs, it can move forward and turn by controlling the motion of different legs [30]. Inspired by inchworms, another insect-scale soft robot has been developed [31]. When the voltage is applied to different actuation regions, the robot can bend/expand or twist its body so that it can run or turn. However, the two insect-scale soft robots can only achieve forward and turning locomotion because their feet can only provide anisotropic friction. Electroadhesive (EA) can adhere to the surface of various objects by applying voltage. This ability can provide friction in any direction as needed. Using EAs as the feet, the mobile robots move in different directions, but only in the plane [27–29]. Inspired by inchworms, an untethered soft robot that can achieve autonomous reciprocated locomotion was developed [4]. The tethered version can turn by applying a voltage to different electrode areas of DEA. Nevertheless, it cannot

* Corresponding authors.
E-mail addresses: liulw@hit.edu.cn (L. Liu), lengjs@hit.edu.cn (J. Leng).

https://doi.org/10.1016/j.eml.2022.101720
2352-4316/© 2022 Elsevier Ltd. All rights reserved.

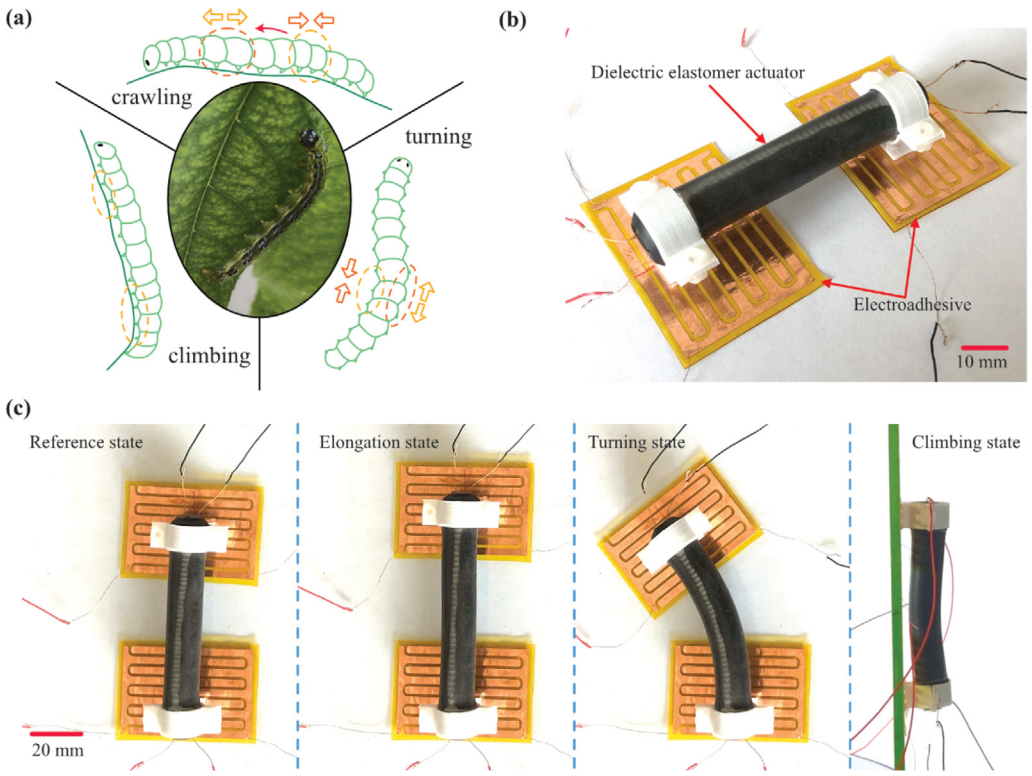

Fig. 1. Caterpillar inspired soft robot. (a) Multimodal locomotion of caterpillars. (b) Prototype of the soft robot. (c) Bioinspired multimodal locomotion of the soft robot. In the reference state, no voltage is applied to the soft robot. In the elongation state, voltage is applied to both sides of the DEA and the lower side EA of the soft robot. In the turning state, voltage is applied to the right side of the DEA and the lower side EA of the soft robot. In the climbing state, voltage is applied to the lower or upper side EA.

climb the wall like an inchworm. Similarly, a soft robot that can climb various walls has also been developed [32]. However, it has to assemble two robots in parallel to be able to turn, which increased the complexity of the structure and control strategy.

To achieve multimodal locomotion like a caterpillar within a simple structure, we developed a soft robot that consists of a two-degrees-of-freedom (2-DOF) DEA as the body and two flexible EAs as the feet, as shown in Fig. 1(b). Based on the simplified locomotion mechanism of caterpillars, the soft robot crawls or turns through the elongation/contraction or bending of the deformable body while the feet provide stable friction. Both DEA and EA were characterized experimentally. We demonstrate that the soft robot could crawl on a plane (2.38 mm/s at 0.8 Hz; movie S1), achieve two turning modes (movie S2), and climb the glass wall (movie S4). Finally, we demonstrate some potential applications, such as carrying a micro camera through the tunnel and crawling on the heat insulation multilayer components on the surface of the satellite (movie S5).

Table 1
Comparison of soft robots driven by dielectric elastomer actuators.

Robot type	Reciprocated crawling	Turning	Climbing	Reference
Inchworm	No	No	No	[19]
	No	No	No	[24]
	No	No	No	[25]
	No	Yes	No	[31]
	Yes	Yes	No	[4]
	Yes	Yes	Yes	[32]
Annelid	No	No	No	[26]
Legged	Yes	No	No	[21]
	No	Yes	No	[30]
Caterpillar	No	No	No	[20]
	Yes	Yes	Yes	This work

2. Materials and methods

2.1. Design of the soft robot

Fig. 2 shows the design of the soft robot. The soft robot is mainly composed of a DEA (robot body) and two EAs (robot feet). The body and feet are connected by two 3D printed actuator holders, as shown in Fig. 2(a). The DEA consists of compressed spring, stretched DE membrane, and end caps. It has 2-degrees-of-freedom (axial elongation/contraction and bidirectional bending), which allows the soft robot to move forward/backward and turn (Fig. 1(c)). EAs were used as the feet to generate stable friction. It consists of a dielectric layer (polyimide, PI), an electrode layer (copper), and an isolation layer (polydimethylsiloxane, PDMS). The ability of EA to adhere to the surface of various objects allows the soft robot to climb the wall (Fig. 1(c)).

Fig. 2(b) shows the control system of the soft robot. Each actuation part was powered by an independent high-voltage amplifier (EMCO A60P-5, XP Power). In order to discharge the actuator safely, a resistor of 100 MΩ was connected in parallel with the actuator. To control the on–off of the power supply for each high-voltage amplifier, 4 MOSFETs were employed and controlled by a microcontroller (Arduino UNO). Fig. 2(c) shows the control strategy and Fig. 2(d) shows the crawling mechanism of the soft robot. First, a voltage was applied to the hind foot, and the adhesion force was generated to anchor the soft robot to the ground. Then the voltage was applied to both sides of the DEA, and the DEA was elongated to make the front foot move forward. Finally, the front foot of the soft robot was anchored to the ground by applying voltage. After the voltage applied to the hind foot and DEA was removed, the DEA contracts and pulls the hind foot

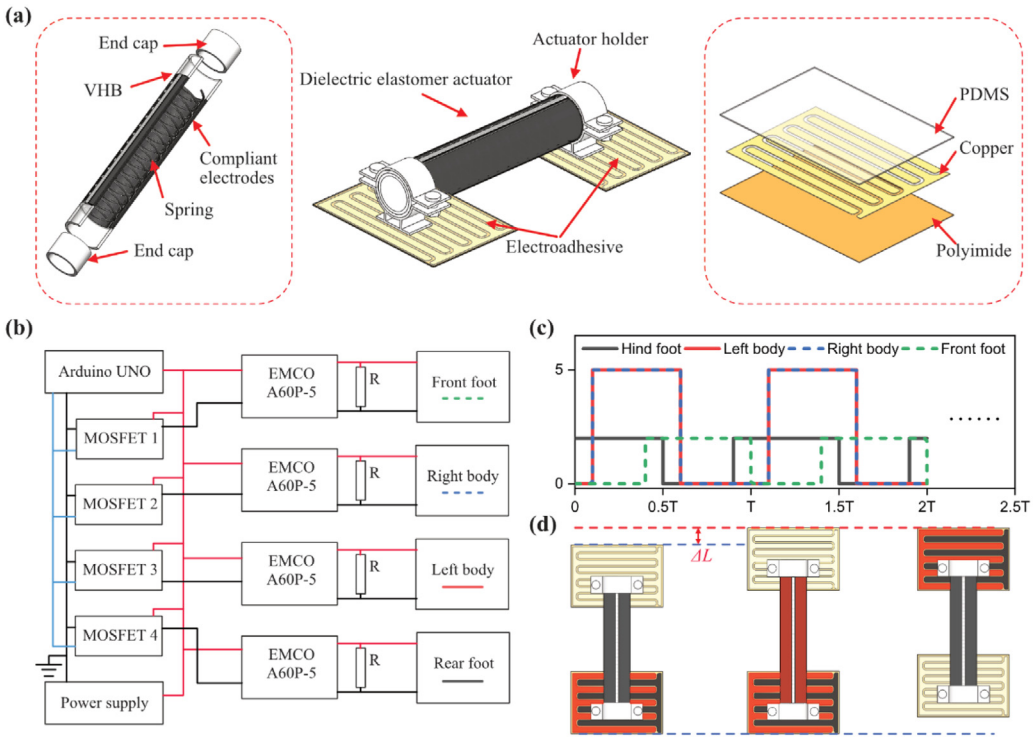

Fig. 2. Design of the soft robot. (a) The soft robot consists of a DEA (left) and two EAs (right). (b) Schematic diagram of the control system of the soft robot. (c) Schematic diagram of the control strategy of the soft robot. (d) Schematic diagram of the crawling mechanism, where red electrodes denote the application of a high voltage and black electrodes denote the ground.. (For interpretation of the references to color in this figure legend, the reader is referred to the web version of this article.)

forward. In this way, the soft robot completes a forward cycle and moves ΔL. If the sequence of applying voltages to the front and hind feet is opposite, the soft robot will move backward. When the voltage applied to the electrodes on both sides of DEA is different, DEA will bend and make the soft robot turn.

2.2. Materials and fabrication

The fabrication process of DEA is illustrated in Fig. 3(a) and could be described as follows. Step 1: The dielectric elastomer membrane (VHB 4910, 3M Company) was pre-stretched biaxially by 3 × 3 and attached to an acrylic frame. Step 2: Carbon grease (846-80G, MG Chemicals) as the compliant electrode was patterned in rectangular shape with a gap of about 2∼3 mm on the one side of the pre-stretched membrane, and copper wire was connected to each electrode for applying high voltage. Step 3: The spring (0.7 mm (wire diameter) × 14 mm (outer diameter) × 180 mm (free length)) was pre-compressed to 70 mm and fixed with end caps at both ends. Step 4: The pre-compressed spring and end caps were rolled over the dielectric elastomer membrane to let the membrane wrap around the spring. There are six layers of effective actuation here. Step 5: To prevent the membrane from slipping off the end caps, heat shrinkable tubes were sleeved at the end caps at both ends.

In this work, a novel low-cost fabrication method was proposed to produce the EA, as shown in Fig. 3(b). The fabrication process can be described as follows. Step 1: The EA was designed in the shape of a comb with an effective area of 52.5 mm × 35 mm. The width of the electrodes is 3 mm and the spacing is 1 mm. Step2: The adhesive copper tape with a thickness of 55 μm was attached to a cutting mat. Then, the copper tape was cut by a cutting machine (Silhouette cameo 4, Silhouette America, Inc.) based on the designed geometry. Step 3 and 4: After the redundant copper tape was removed, the EA left behind was transferred to the 30 μm thick polyimide (PI) film with transfer paper. The use of transfer paper ensures that the shape of the EA does not change during the transfer process. Copper wires were connected to the electrodes for applying high voltage. Step 5: The polydimethylsiloxane (PDMS, Sylgard 184, Dow Corning) was used as the dielectric material to prevent EA breakdown in the air. It was mixed in a weight ratio of 1:10 and scraped on the EA surface. Then, it was cured at 60 °C for 2 h. Finally, the effective EA was cut out for testing.

For the soft robot, a connecting structure is also needed to connect the body and feet. The structure was made easily by 3D printing based on the designed model. Then, we can assemble the various parts of the soft robot, as shown in Fig. 3(c). The DEAs were fixed by connecting structures, and then VHB 4910 was used to bond the connecting structures and EAs together. This “modular” approach also makes the replacement of damaged parts of the soft robot more convenient.

2.3. Characterization method

Both the deformation and output force of DEA were characterized. When testing the bending angle as a function of voltage, one end of DEA was fixed by the actuator holder and the other end is free, as shown in Fig. 4(a). A high-voltage amplifier (EMCO Q80-5, XP Power) was used to drive DEA. The measurement steps can be described as follows. Step 1: Initially, a step voltage was applied to one side of the DEA. Step 2: After 4 s, the voltage was removed and the next test was carried out after DEA returns to the initial state. The whole process was recorded by video to obtain the bending angle. The test voltage ranges from 4 kV to 6.5 kV with a step value of 0.5 kV, and each voltage was repeated three times to obtain the average value. The same approach was used to test the axial displacement, but the differences were that the voltage was applied to both sides of DEA at the same time,

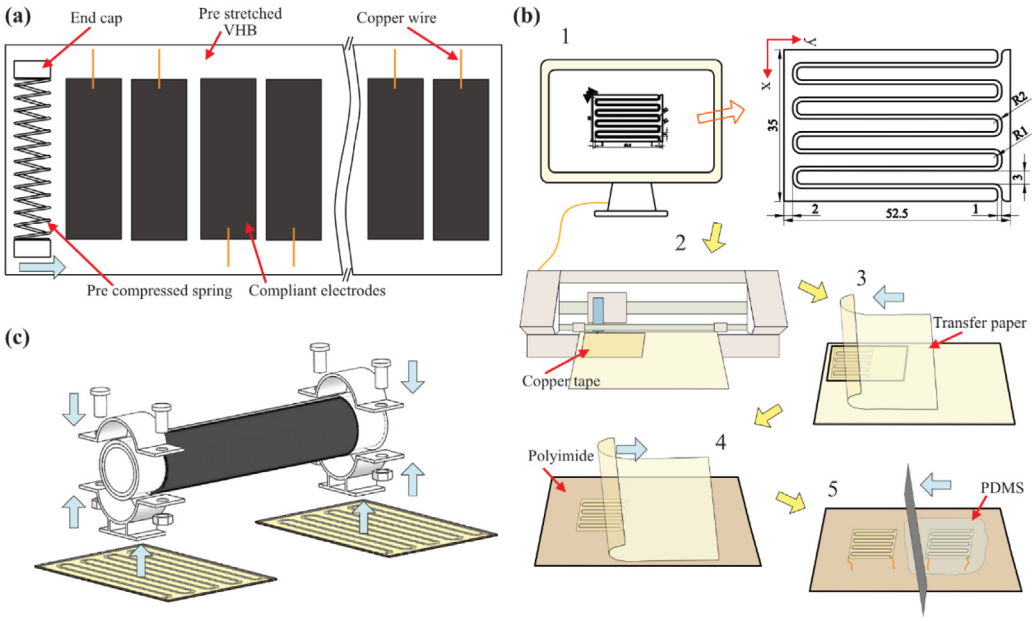

Fig. 3. Fabrication of the soft robot. (a) Schematic diagram of the 2-DOF DEA fabrication. (b) Schematic diagram of the EA fabrication. (c) Assembly of the soft robot.

and the displacement was recorded by laser displacement sensor (HG-C1050, Panasonic).

When testing the blocking force with the change of bending angle, one end of the DEA was fixed on the actuator holder and the load cell (LDCAL-SD) was fixed vertically at the other end. A data acquisition equipment (USB 6002, NI) was used to record data. At the beginning, a step voltage was applied to one side of DEA, and the voltage was removed after holding for 4 s. The maximum force generated was used as the lateral blocking force. The test was carried out every 10° until the lateral blocking force was less than 0. For the axial blocking force of DEA with the change of axial displacement, one end of DEA was fixed on the platform, and the other end was connected with the load cell. The measurement obeys the following steps. Step 1: At the beginning, a step voltage was applied to both sides of the DEA. Step 2: After 4 s, the load cell fixed on the linear rail moved 1 mm at a constant speed of 0.25 mm/s, then stops for 4 s. Step 3: This process was repeated until the axial blocking force was less than 0. Each load condition was repeated three times to obtain the average value.

The electroadhesion forces in two directions were tested. As shown in Fig. 4(b), the EA placed on the glass substrate was connected to the load cell. The measurement steps can be described as follows. Step 1: At the beginning, the load cell was pulled by the linear rail to move 5 mm at a constant speed of 0.1 mm/s to test the initial static friction of the EA. Step 2: After stopping, a step voltage was applied to EA, hold for 5 s, and then move 5 mm at the same speed of 0.1 mm/s. The maximum force in this process minus the initial static friction force was set as the shear adhesive force of EA. All the tests were conducted at room temperature of 24.3 ± 0.1 °C and humidity of 49 ± 2%. The test voltage ranges from 2 kV to 3.5 kV with a step value of 0.5 kV. The tests were repeated three times for each voltage to obtain the average value and each test was separated by 5 min to allow the EA to be fully discharged.

3. Results and discussions

3.1. Actuation performance of the DEA and EA

First, we characterized the effect of the applied voltage on the performance of 2-DOF DEA. In the absence of voltage, DEA

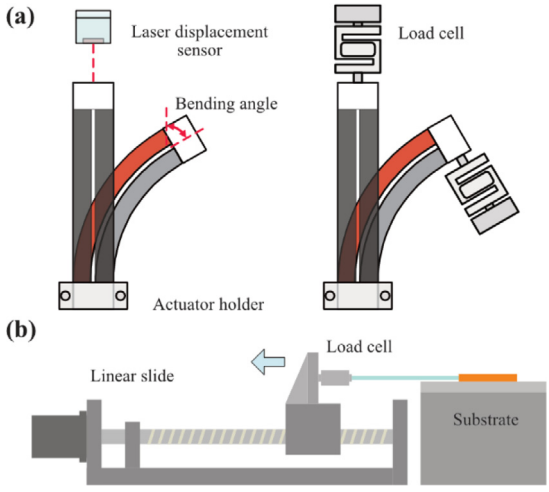

Fig. 4. Characterization platforms for the soft robot. (a) Schematic diagram of displacement, bending angle, and force test of the DEA. (b) Schematic diagram of shear adhesive force test of the EA.

is straight and has an initial length. When a voltage is applied to one side of the DEA, that side will elongate and the other side will remain unchanged, causing the DEA to bend to the opposite side and vice versa. If both sides of the DEA are powered on simultaneously, the DEA will elongate along the axial direction. When the voltage is removed, DEA returns to its initial state. Such deformations enable the soft robot to crawl and turn. As shown in Fig. 5(a), with the increase of voltage, the axial displacement and bending angle increase gradually. When the voltage is 6.5 kV, the axial displacement and bending are 16.5 mm and 108° respectively. It is also noted that the bending angles on both sides are slightly different, which should be caused by manual errors.

When the soft robot crawls, it needs to overcome the friction between its feet and the substrate to elongate and contract its body. In addition, it also needs to overcome gravity when climbing the wall. The output force of DEA has a crucial influence on crawling. Fig. 5(b) and (c) show the variation of axial force with axial displacement and lateral force with bending angle at

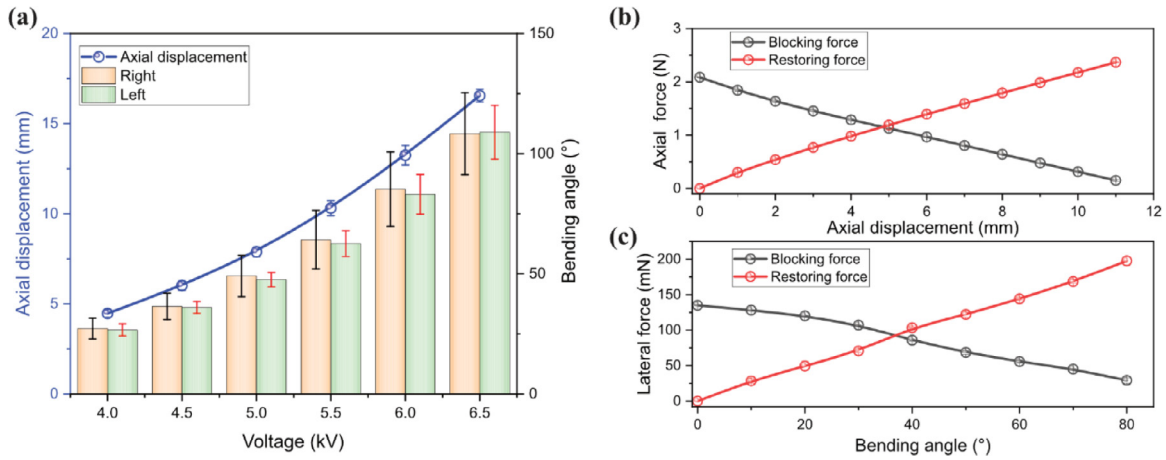

Fig. 5. Performance of the DEA. (a) The axial displacement and bending angle of the DEA under different voltages. (b) The axial force under different axial displacements. (c) The lateral force under different bending angles.

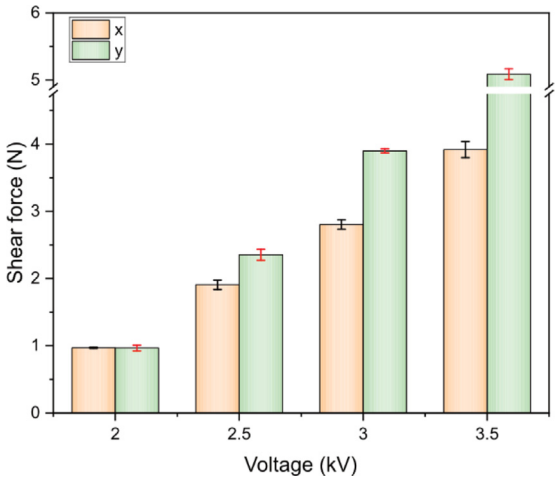

Fig. 6. The shear adhesive force in x and y directions under different voltages.

5.5 kV respectively. With the increase of the deformation (axial displacement or bending angle) of the DEA, the blocking force (axial force or lateral force) of the DEA decreases monotonically. The restoring force shows the opposite trend.

When the voltage is applied to the EA placed on the dielectric substrate, the charges accumulated on the electrode and the charges generated on the substrate due to dielectric polarization attract each other, resulting in electrostatic forces. This provides the necessary friction for the locomotion of the soft robot. Fig. 6 shows the change of shear adhesive force of EA with voltage. With the increase of voltage, the shear adhesive force of EA increases gradually, and the difference between the two directions is also increasing. When the voltage is 3.5 kV, the shear adhesive force in x-direction reaches 3.9 N. Meanwhile, it should be pointed out that the shear adhesive force in y-direction has exceeded the range of the load cell, so this is not an accurate value.

3.2. Crawling results

Fig. 7 shows the crawling results of the soft robot. Fig. 7(a) shows the process of the soft robot moving forward at a frequency of 0.8 Hz. The actual voltage of each driving part when the soft robot moves forward at a frequency of 0.2 Hz is shown in Fig. 7(b). The capacitances of DEA and EA are 32.7 pF and 6.8 pF, respectively. Therefore, the electrical energy can be estimated by $U = C \times V^2/2$ based on the measured capacitances and voltages. The total electrical energy consumption for each cycle of the soft robot is 1.02 mJ. It also shows the control strategy in detail. When the voltage applied to EA was removed, the electrostatic force decreases rapidly. In order to achieve more stable crawling, especially to prevent falling off when climbing the wall, the voltages applied to the front and hind feet overlap for one-fifth of half a cycle.

The crawling speed of the soft robot at different frequencies is shown in Fig. 7(c). At 0.8 Hz, its crawling speed reaches the maximum value of 2.38 mm/s, corresponding to 0.022 body length per second (BL/s), but this is not the maximum crawling speed it can achieve. In order to ensure the safety of DEA and high voltage amplifier, the voltage was limited to 5.5 kV. DEA has better performance at higher voltage, as shown in Fig. 5(a). In addition, the control system also limits the soft robot to work at higher frequencies. As shown in Fig. 8(b), the change of applied voltage at 0.8 Hz. Due to the shortening of the time of each cycle, the discharge is not sufficient, thus the DEA cannot fully recover. The existence of residual charge makes the electrostatic force further hinder the deformation of DEA. Therefore, the deformation of DEA in each cycle is reduced.

Lifetime is a key parameter of soft robots. In the crawling experiment, the lifetime of the soft robot was tested. The soft robot crawled continuously for more than 2 h in one test. It remained functional after more than 10 000 operation cycles.

3.3. Turning results

Natural creatures such as caterpillars and inchworms can turn by bending their bodies, which is a key ability for survival. Currently, few soft robots based on DEAs have the ability to turn, as shown in Table 1. The soft robot in this work can achieve two turning modes due to the 2-DOF characteristics of DEA, as shown in Fig. 8. As described in Section 2.1, each actuation part of the soft robot was driven by an independent high voltage amplifier, so the voltage can be adjusted independently. When different voltages are applied to the electrodes on both sides of the DEA (Fig. 8(b)), due to the different elongation on both sides, the DEA will bend while elongating, so that it can turn when crawling forward (see Fig. 8(a) and movie S2). In addition, the ability to adjust the voltage independently has another advantage. Due to the manual error, the elongation on both sides of some DEA is different under the same voltage. Therefore, the influence caused by this part can be eliminated by adjusting the voltage, so that the soft robot can crawl in a straight line. Fig. 8(c) shows the turning

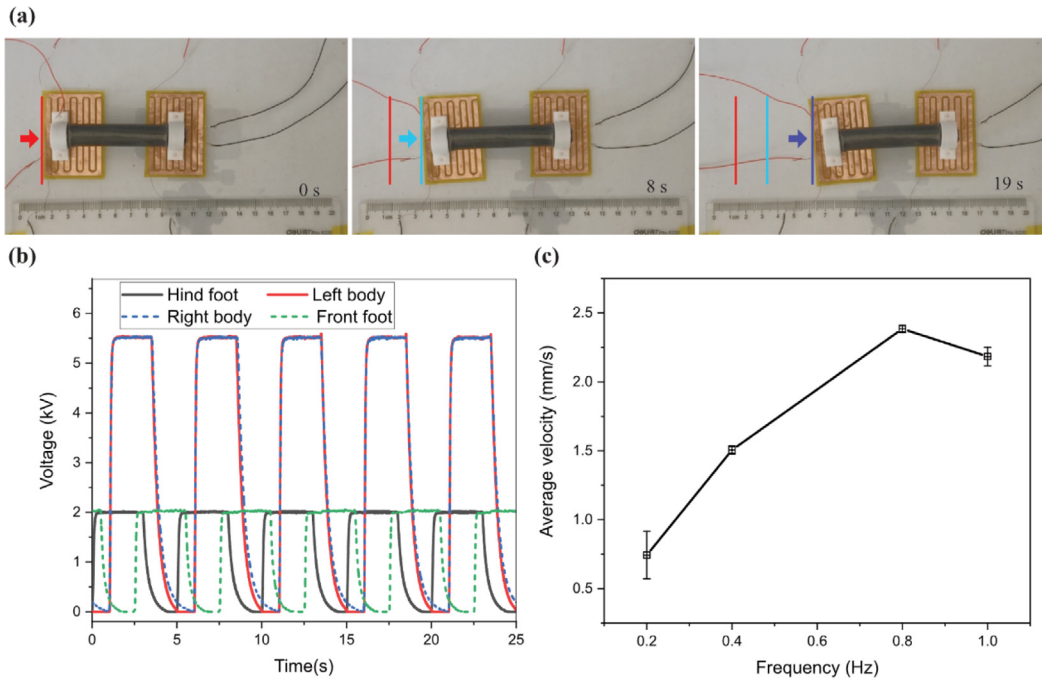

Fig. 7. Crawling results of the soft robot (See movie S1). (a) Crawling process of the soft robot at 0.8 Hz. (b) The actual voltage applied to the robot in the forward crawling experiment. (c) The movement speed of the robot at different frequencies.

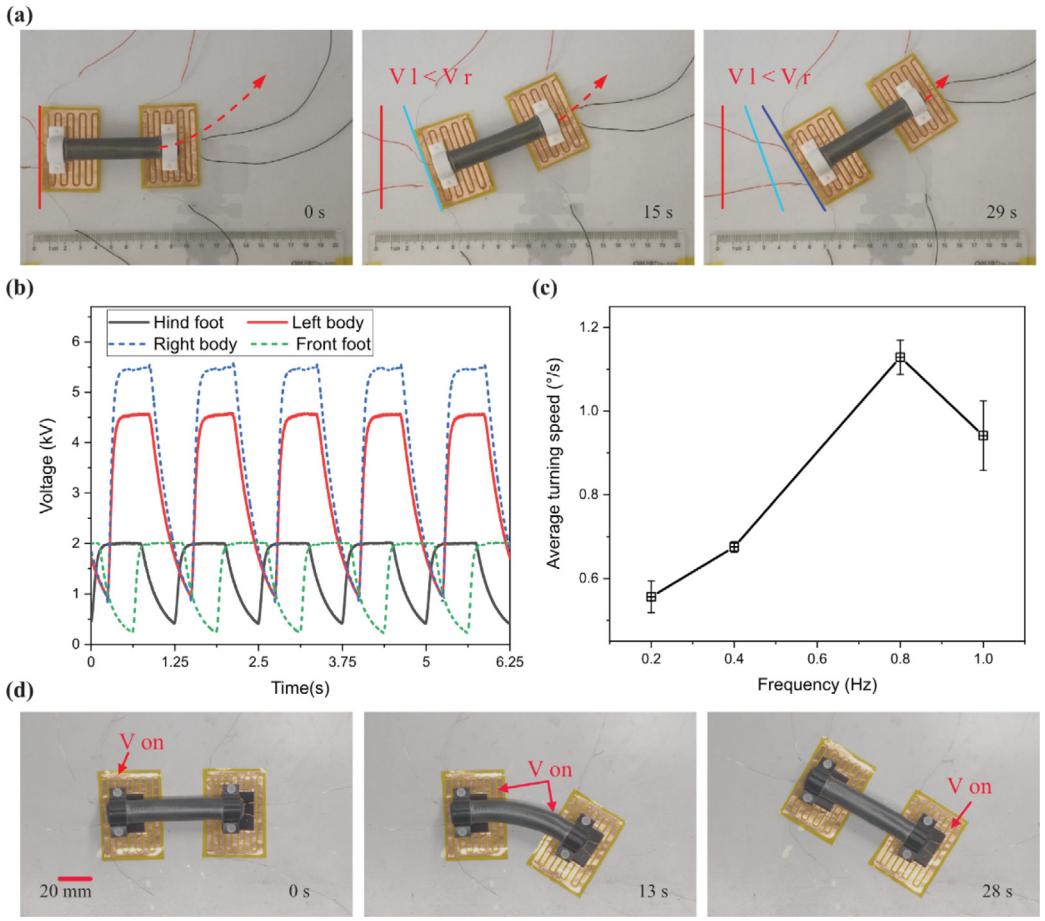

Fig. 8. Turning results of the soft robot (See movie S2). (a) Turn mode 1. (b) The actual voltage applied to the robot in the turning experiment. (c) The turning speed at different frequencies. (d) Turn mode 2.

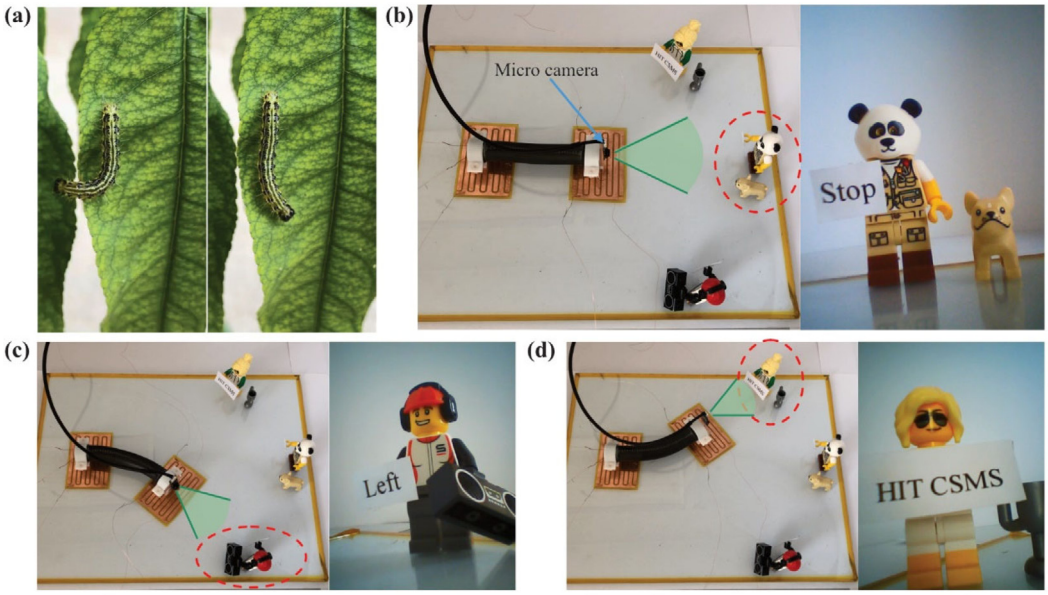

Fig. 9. The caterpillar inspired looking-around locomotion (See movie S3). (a) A caterpillar on the leaf looks around. (b) The soft robot looks forward through the micro camera. (c) The soft robot looks to the right by bending its body. (d) The soft robot looks to the left by bending its body.

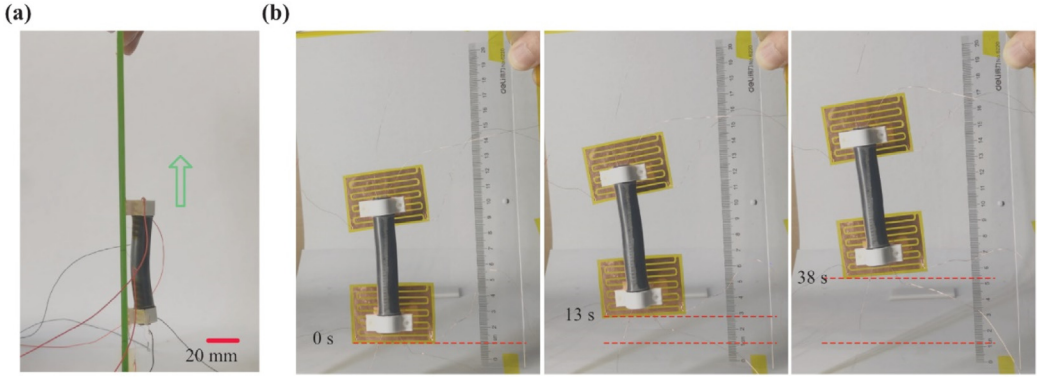

Fig. 10. Climbing a glass wall (See movie S4). (a) Side view of the glass wall climbing. (b) Front view of the glass wall climbing at 0.8 Hz.

speed of the soft robot at different frequencies and the maximum turning speed is 1.1°/s at 0.8 Hz.

Fig. 8(d) shows another turning mode, which will have more advantages in the narrow space. When the hind foot anchored to the ground by applying voltage, only one side of the DEA is electrified to make the DEA bend at a large angle. Then, the front foot anchored to the ground by applying voltage, and the voltages applied to the hind foot and the body were removed to make the body straight again, completing a turning process. Since the lateral force of DEA is relatively small (Fig. 5(b)) and the electrostatic force of EA needs a long time to be eliminated, it is difficult for the soft robot to return to the straight state after the voltages were removed. Therefore, it is possible to apply voltage to the other side of the DEA while removing the voltages applied to the hind foot and one side of the body to make the body of the soft robot straighten quickly or bend in the opposite direction. By repeating the above control strategy, the soft robot can turn in a small space (see movie S2).

In addition, this way of bending the body also allows the soft robot to imitate the looking-around locomotion of caterpillars (see movie S3). As shown in Fig. 9, a micro camera (HBV - 1319, Huiber Vision Technology Co. LTD.) was fixed on the robot to act as its eye. When the hind foot anchored to the ground, the soft robot can inspect the surroundings by bending the body (Fig. 9(c) and (d)), just like a caterpillar looking around (Fig. 9(a)).

3.4. Climbing results

Wall climbing has always been a challenge for soft robots, although it is common for natural creatures. In this work, the soft robot has the ability to climb the wall because EAs are employed as the feet. The climbing mechanism is the same as that in-plane crawling. The total mass of the soft robot is about 12 g. For stable climbing, the voltage applied to the feet was increased from 2 kV to 2.5 kV to avoid sliding. Fig. 10 shows the climbing result of the soft robot. For the soft robot, the maximum speed of climbing the glass wall is almost the same as that of crawling in the plane, reaching 2.3 mm/s (0.021 BL/s).

Table 2 shows the performance comparison of soft robots driven by dielectric elastomer actuators. The symbol of/ in the table indicates that the soft robot did not have this locomotion mode, and N/A indicates that no specific value was reported. Although our soft robot has almost no advantage in crawling speed compared with other soft robots, it can achieve turning and climbing locomotion modes, which cannot be realized by many other soft robots. In addition, our soft robot also has a more compact structure compared with the soft robot in literature [32].

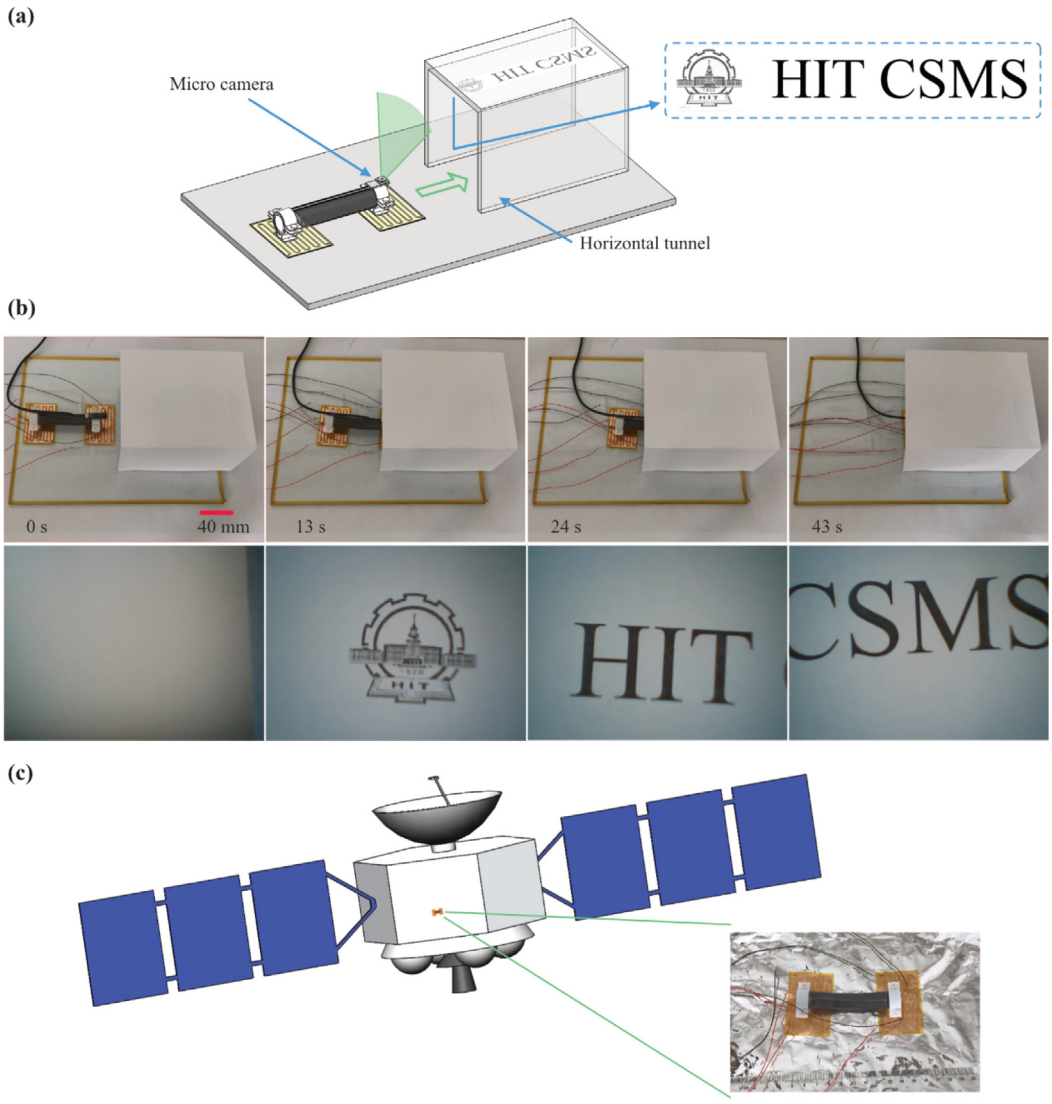

Fig. 11. Applications of the soft robot (See movie S5). (a) Schematic illustration of the inspection function in a confined horizontal tunnel. (b) Front view and video recording process of the soft robot. (c) Schematic illustration of the soft robot on a satellite and front view of the robot crawling on a heat insulation multilayer component.

Table 2
Comparison of locomotion speed of soft robots driven by dielectric elastomer actuators.

Robot type	Crawling speed (BL/s)	Turning speed (°/s)	Climbing speed (BL/s)	Reference
Inchworm	1.03	/	/	[24]
	0.022	/	/	[25]
	2.75	N/A	/	[31]
	0.02	N/A	/	[4]
	1.04	62.79 (two DEA units were used)	0.75	[32]
Annelid	0.031	/	/	[26]
Legged	0.2	/	/	[21]
	0.3	30 (three DEA units were used)	/	[30]
Caterpillar	0.022	1.1 (only one DEA was used)	0.021	This work

3.5. Applications of the soft robot

Here, we demonstrate some potential applications of this soft robot. As shown in Fig. 11(a), a micro camera was fixed on the robot, so that it can record the video while crawling. When crossing the confined horizontal tunnel (length, 140 mm; width, 115 mm; height, 85 mm), the image and letters "HIT CSMS" on the top wall of the tunnel were recorded (Fig. 11(b) and movie S5).

In addition, the soft robot also has the potential for exploration and inspection. EA can adhere to the surface of many materials when voltage is applied. Heat insulation multilayer components are commonly used in spacecraft, such as satellites and space stations to keep the temperature within a certain range. Fig. 11(c)

demonstrated the crawling capabilities of the soft robot on the heat insulation multilayer components (see movie S5).

4. Conclusions

In summary, we have developed a caterpillar inspired soft robot with a 2-DOF DEA as the deformable body and 2 flexible EAs as the feet. The DEA can be used to elongate 16.5 mm along the axial direction or bend 108° to both sides when the voltage was 6.5 kV. The EA can be used to generate 3.9 N shear adhesive force when the voltage was 3.5 kV. The soft robot capable of multimodal locomotion, including crawling (2.38 mm/s at 0.8 Hz), turning (1.1°/s at 0.8 Hz), and climbing walls (maximum speed of 2.3 mm/s at 0.8 Hz), has been demonstrated. Over 10 000 operation cycles were obtained. In addition, the soft robot carried a micro camera and walked through the horizontal tunnel and can be used to crawl on the heat insulation multilayer components.

Although the soft robot has achieved a variety of locomotion modes, there are still many challenges for practical applications. For example, the soft robot can only crawl in a plane. We will explore the possibility of using a 3-DOF DEA as the body of the soft robot. In this way, the body of the soft robot can bend in multiple directions to adapt to the more complex curved surfaces, and even crawl from a horizontal plane to a vertical wall. It can also lift its head like a natural creature to observe its surroundings. This will greatly expand the application of the soft robot. In addition, we will increase the output force of the DEA and EA so that the soft robot can carry more loads. Therefore, an untethered version of the soft robot can be achieved.

Declaration of competing interest

The authors declare that they have no known competing financial interests or personal relationships that could have appeared to influence the work reported in this paper.

Acknowledgment

This work is supported by the National Natural Science Foundation of China (Grant No. 11772109).

Appendix A. Supplementary data

Supplementary material related to this article can be found online at https://doi.org/10.1016/j.eml.2022.101720.

References

[1] G.Y. Gu, J. Zhu, L.M. Zhu, X. Zhu, A survey on dielectric elastomer actuators for soft robots, Bioinspiration Biomim. 12 (2017) 011003.
[2] S. Chen, Y. Cao, M. Sarparast, H. Yuan, L. Dong, X. Tan, C. Cao, Soft crawling robots: design, actuation, and locomotion, Adv. Mater. Technol. 5 (2019) 1900837.
[3] Y.G. Guo, L.W. Liu, Y.J. Liu, J.S. Leng, Review of dielectric elastomer actuators and their applications in soft robots, Adv. Intell. Syst. 3 (2021) 2000282.
[4] J. Cao, L. Qin, J. Liu, Q. Ren, C.C. Foo, H. Wang, H.P. Lee, J. Zhu, Untethered soft robot capable of stable locomotion using soft electrostatic actuators, Extreme Mech. Lett. 21 (2018) 9–16.
[5] T. Lu, C. Ma, T. Wang, Mechanics of dielectric elastomer structures: A review, Extreme Mech. Lett. 38 (2020) 100752.
[6] G.M. Whitesides, Soft robotics, Angew. Chem. Int. Edn 57 (2018) 4258–4273.
[7] D. Rus, M.T. Tolley, Design, fabrication and control of soft robots, Nature 521 (2015) 467–475.
[8] H.T. Lin, G.G. Leisk, B. Trimmer, GoQBot: a caterpillar-inspired soft-bodied rolling robot, Bioinspiration Biomim. 6 (2011) 026007.
[9] S. Seok, C.D. Onal, K.-J. Cho, R.J. Wood, D. Rus, S. Kim, Meshworm: a peristaltic soft robot with antagonistic nickel titanium coil actuators, IEEE/ASME Trans. Mechatronics 18 (2013) 1485–1497.
[10] J.S. Leng, X. Lan, Y.J. Liu, S.Y. Du, Shape-memory polymers and their composites: Stimulus methods and applications, Prog. Mater. Sci. 56 (2011) 1077–1135.
[11] Q. Peng, H. Wei, Y. Qin, Z. Lin, X. Zhao, F. Xu, J. Leng, X. He, A. Cao, Y. Li, Shape-memory polymer nanocomposites with a 3D conductive network for bidirectional actuation and locomotion application, Nanoscale 8 (2016) 18042–18049.
[12] Y. Qiu, E. Zhang, R. Plamthottam, Q. Pei, Dielectric elastomer artificial muscle: materials innovations and device explorations, Acc. Chem. Res. 52 (2019) 316–325.
[13] L.J. Romasanta, M.A. Lopez-Manchado, R. Verdejo, Increasing the performance of dielectric elastomer actuators: A review from the materials perspective, Prog. Polym. Sci. 51 (2015) 188–211.
[14] I. Must, F. Kaasik, I. Põldsalu, L. Mihkels, U. Johanson, A. Punning, A. Aabloo, Ionic and capacitive artificial muscle for biomimetic soft robotics, Adv. Energy Mater. 17 (2015) 84–94.
[15] T.J. White, D.J. Broer, Programmable and adaptive mechanics with liquid crystal polymer networks and elastomers, Nature Mater. 14 (2015) 1087–1098.
[16] C. Wang, K. Sim, J. Chen, H. Kim, Z. Rao, Y. Li, W. Chen, J. Song, R. Verduzco, C. Yu, Soft ultrathin electronics innervated adaptive fully soft robots, Adv. Funct. Mater. 30 (2018) 1706695.
[17] X. Zhao, Multi-scale multi-mechanism design of tough hydrogels: building dissipation into stretchy networks, Soft Matter 10 (2014) 672–687.
[18] X. Du, H. Cui, T. Xu, C. Huang, Y. Wang, Q. Zhao, Y. Xu, X. Wu, Reconfiguration, camouflage, and color-shifting for bioinspired adaptive hydrogel-based millirobots, Adv. Funct. Mater. 30 (2020) 1909202.
[19] J. Li, L. Liu, Y. Liu, J. Leng, Dielectric elastomer spring-roll bending actuators: applications in soft robotics and design, Soft Robot. 6 (2019) 69–81.
[20] E.M. Henke, S. Schlatter, I.A. Anderson, Soft dielectric elastomer oscillators driving bioinspired robots, Soft Robot. 4 (2017) 353–366.
[21] C.T. Nguyen, H. Phung, T.D. Nguyen, H. Jung, H.R. Choi, Multiple-degrees-of-freedom dielectric elastomer actuators for soft printable hexapod robot, Sensors Actuators A 267 (2017) 505–516.
[22] C.T. Nguyen, H. Phung, P.T. Hoang, T.D. Nguyen, H. Jung, H. Moon, J.C. Koo, H.R. Choi, A novel bioinspired hexapod robot developed by soft dielectric elastomer actuators, in: 2017 IEEE/RSJ International Conference on Intelligent Robots and Systems (IROS), 2017, pp. 6233–6238.
[23] J. Zhao, J. Zhang, D. McCoul, Z. Hao, S. Wang, X. Wang, B. Huang, L. Sun, Soft and fast hopping-running robot with speed of six times its body length per second, Soft Robot. 6 (2019) 713–721.
[24] M. Duduta, D.R. Clarke, R.J. Wood, A high speed soft robot based on dielectric elastomer actuators, in: 2017 IEEE International Conference on Robotics and Automation (ICRA), 2017, pp. 4346–4351.
[25] S. Shian, K. Bertoldi, D.R. Clarke, Use of aligned fibers to enhance the performance of dielectric elastomer inchworm robots, in: Electroactive Polymer Actuators and Devices (EAPAD) 2015, 2015, p. 94301P.
[26] L. Xu, H.Q. Chen, J. Zou, W.T. Dong, G.Y. Gu, L.M. Zhu, X.Y. Zhu, Bio-inspired annelid robot: a dielectric elastomer actuated soft robot, Bioinspiration Biomim. 12 (2017) 025003.
[27] K.M. Digumarti, C. Cao, J. Guo, A.T. Conn, J. Rossiter, Multi-directional crawling robot with soft actuators and electroadhesive grippers, in: 2018 IEEE International Conference on Soft Robotics (RoboSoft), 2018, pp. 303–308.
[28] L. Qin, Y. Tang, U. Gupta, J. Zhu, A soft robot capable of 2D mobility and self-sensing for obstacle detection and avoidance, Smart Mater. Struct. 27 (2018) 045017.
[29] W. Li, W. Zhang, H. Zou, Z. Peng, G. Meng, Multisegment annular dielectric elastomer actuators for soft robots, Smart Mater. Struct. 27 (2018) 115024.
[30] X. Ji, X. Liu, V. Cacucciolo, M. Imboden, Y. Civet, A.E. Haitami, S. Cantin, Y. Perriard, H. Shea, An autonomous untethered fast soft robotic insect driven by low-voltage dielectric elastomer actuatorsl, Science Robotics 4 (2019) eaaz6451.
[31] T. Li, Z. Zou, G. Mao, X. Yang, Y. Liang, C. Li, S. Qu, Z. Suo, W. Yang, Agile and resilient insect-scale robot, Soft Robot. 6 (2018) 133–141.
[32] G. Gu, J. Zou, R. Zhao, X. Zhao, X. Zhu, Soft wall-climbing robots, Science Robotics 3 (2018).